LEED holography applied to a complex superstructure: a direct view of the adatom cluster on SiC(111)-(3×3)

K. Reuter, J. Schardt, J. Bernhardt, H. Wedler, U. Starke and K. Heinz
Lehrstuhl für Festkörperphysik, Universität Erlangen-Nürnberg, Staudtstr. 7, D-91058 Erlangen, Germany

For the example of the SiC(111)-(3×3) reconstruction we show that a holographic interpretation of discrete Low Energy Electron Diffraction (LEED) spot intensities arising from ordered, large unit cell superstructures can give direct access to the local geometry of a cluster around an elevated adatom, provided there is only one such prominent atom per surface unit cell. By comparing the holographic images obtained from experimental and calculated data we illuminate validity, current limits and possible shortcomings of the method. In particular, we show that periodic vacancies such as cornerholes may inhibit the correct detection of the atomic positions. By contrast, the extra diffraction intensity due to slight substrate reconstructions, as for example buckling, seems to have negligible influence on the images. Due to the spatial information depth of the method the stacking of the cluster can be imaged down to the fourth layer. Finally, it is demonstrated how this structural knowledge of the adcluster geometry can be used to guide the dynamical intensity analysis subsequent to the holographic reconstruction and necessary to retrieve the full unit cell structure.

PACS-numbers: 61.14.Nm, 61.10.Dp, 61.14.Hg, 68.35.Bs **Phys. Rev. B, (1998)** *in press*

I. INTRODUCTION

The majority of ordered surface structures known today has been determined by Low Energy Electron Diffraction (LEED)[1]. The strong elastic and inelastic interaction of electrons in the energy range 50-500eV involves a particular sensitivity to the atomic arrangement within the outermost layers. In many cases this permits a structure determination with a precision of a few hundredths of an Ångstrøm, making LEED one of the primary surface crystallography methods. Unfortunately, the strong multiple scattering implied by this type of interaction also tremendously complicates the theoretical analysis of the acquired data. In addition, the real space geometry can not be drawn from the intensities directly, so that standard quantitative LEED structure determinations have to apply a trial-and-error method which is frequently supported by structural search procedures. Calculated diffraction intensities of a multitude of models have to be compared with the experimental data until eventually a sufficiently high agreement between both is achieved[2–4].

Though more and more advanced experimental and theoretical developments have recently given access to rather complex surface structures[4], it is just this complexity which at a certain degree inhibits the successful application of quantitative LEED. The number of models as resulting from the mere combination of all coordinates of the many atoms in a large unit cell structure becomes so huge that it is difficult if not impossible to handle. This applies even when for example using automated search algorithms in multi-parameter space[5] as the latter has to include the correct model. However, for a large unit cell structure our structural imagination is frequently unable to even define the type of the correct model or the relevant part of the parameter space containing the real structure, in which a search could then be started. Also, methods developed in LEED to determine the atomic positions directly still rely on an initial good guess of the real structure[6].

The holographic approach represents a revival of the hope for the *direct* disclosure of structural information. The idea, first developed for the related Photoelectron Diffraction[7,8], aims at the determination of at least partial features of the structure when in addition to the multiple scattering problem the complexity of the surface prohibits its full retrieval. In the present case, the information provided consists of the local environment around an elevated atom in the cell, which might be an adsorbate or an intrinsic adatom resulting from surface restructuring. Even though only some atomic positions at a rather coarse resolution are determined in this manner, the necessary consistency of the obtained structural unit with the complete surface geometry may rule out many models directly. Hence, the remaining parameter space can be reduced to an extent sufficient to allow the application of conventional surface crystallography methods.

The first translation of holographic schemes to the field of LEED as proposed by Saldin and De Andres[9] was restricted to surfaces on which atoms or molecules are adsorbed in lattice gas disorder. The lacking periodicity creates diffraction intensity also outside the sharp substrate Bragg spots and causes a diffuse intensity distribution on the screen (for a recent review on Diffuse LEED (DLEED) see e.g. ref. 10). This appeared as the natural input for the Fourier-like integral transform typical for holographic techniques. In the course of subsequent theoretical improvements a proper reconstruction algorithm could be established that allowed to circumvent several problems complicating the holographic interpretation of LEED intensities (see section II). In the present investigation we use the latest stage of this development which allows to construct a reliable image of the complete 3D

atomic surrounding of the elevated atom from data of normal incidence alone[11–13].

However, these theoretical achievements were based on the use of diffuse intensity distributions emerging from disordered systems while the majority of interesting surface structures are ordered phases, often with large superstructure unit cells. Certainly, it would be very advantageous to obtain a partial, but *direct* information by holographic means for these *ordered* phases, too. As we briefly demonstrated recently[14], the diffraction intensities arising from this class of systems may be used as input to just the same holographic reconstruction algorithm as developed for the DLEED case. Two important restrictions for this type of application have to be mentioned: there must be only one elevated adatom per surface unit cell and the unit cell must have a minimum size. The first condition arises from the necessity of a unique holographic reference wave as we will outline in the third section. The second limit is based on the data density available and required. The approximate minimum size of the unit cell could recently be estimated as a p(2×2) mesh[15]. An upper size limit is drawn by experimental factors and the more likely appearance of several adatoms per unit cell with increasing unit cell area. A (7×7) cell already appears to be too large as discussed in section III.

Still, a considerable number of ordered reconstructions remains open for a holographic analysis. In the present paper, our investigations are focused on the first successful application to an ordered and *a priori* unknown complex structure case, the example of the SiC(111)-(3×3) superstructure. This surface phase is of considerable interest in current crystal growth investigations[16] of the promising semiconductor material SiC[17]. Previous STM work[18–20] had revealed a single large protrusion per surface unit cell. So, this reconstruction seemed particularly suited for a first application of holographic LEED to ordered surfaces meeting both requirements outlined above, i.e. sufficient unit cell size and the presence of a single elevated atom. By comparing the holographic images obtained from experimental data and from calculated intensities for fictitious models deviating from the real surface geometry we illuminate new aspects of the validity and possible shortcomings of the new method.

The paper is organized as follows: in the next section we recall the holographic reconstruction algorithm using diffuse LEED intensities. Thereafter we describe the relation between diffuse and discrete intensities and give arguments under which circumstances the holographic algorithm may readily be applied to conventional spot intensities. This is followed by the reconstruction of an atomically well resolved image from the experimental LEED intensities measured for the SiC(111)-(3×3) phase. Section V shows that the spatial depth accessible by the method is rather large, which allows to determine such important features as the stacking sequence of deeper layers. In section VI, we illuminate the role of periodic vacancies within the unit cell acting as additional

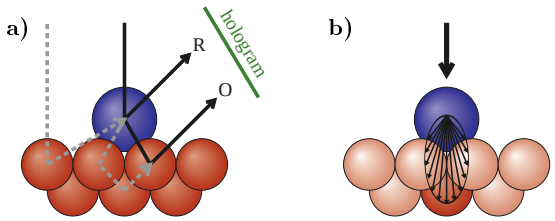

FIG. 1. Schematic display of the holographic interpretation of the adatom scattering: a) electrons finally scattering at the adatom form the *reference* wave R, those subsequently hitting one substrate atom represent the kinematic *object* wave O (solid lines). The dashed lines display possible multiple scattering events providing dynamic contributions to the reference and object wave (see text for details). b) Pronounced forward scattering at the beam-splitter indicated by different length of the arrows in different directions.

holographic reference waves. Then we address the issue of intensities arising from substrate relaxations such as buckling and finally discuss the use of the holographic information for a complete surface structure analysis in the case of SiC(111)-(3×3), whose precise real space structure is described in more detail elsewhere[21,22].

II. THE HOLOGRAPHIC RECONSTRUCTION ALGORITHM

The holographic approach in DLEED makes use of the fact, that all measurable diffuse intensity outside the sharp substrate Bragg spots necessarily has been caused by at least one scattering event at one of the disordered adsorbates on top of the (unreconstructed) crystal: scattering exclusively within an ideal bulk-terminated substrate can only lead to diffraction intensities at Bragg spot positions. In that sense the adsorbate atom can be viewed as a prominent scatterer which, acting as a beam-splitter, provides a natural separation of all scattering paths as depicted by the solid lines in Fig. 1(a): electrons whose final scattering is by an adsorbate form the *reference* wave $R(\mathbf{k})$, while those scattered subsequently by substrate atoms before reaching the detector provide the *object* wave $O(\mathbf{k})$[9] (where $\mathbf{k} \equiv (\mathbf{k}_\parallel, k_\perp)$ is the wavevector of the detected electron, with the components $\mathbf{k}_\parallel$ parallel to, and $k_\perp$ perpendicular to the surface). This allows to interprete the diffuse intensity as the interference pattern of these two contributions. Hence, the local surrounding of the beam-splitter atom should be extractable by a phased 2D Fourier transform of the data[8,9]. However, the above interpretation does not include that multiple scattering adds unwanted contributions to both reference and object wave as indicated in Fig. 1(a) by the dashed lines. A considerable improvement in the image quality could

be achieved by combining several DLEED patterns measured at different electron energies[23]. The corresponding multi-energy reconstruction algorithms include a 3D integral transform and try to single out the contributions due to the kinematic object wave, suppressing the unwanted effects caused by the multiple scattering of the low energy electrons.

Yet, the pronounced forward scattering of the beam-splitter led to only a selective appearance of the atoms in the reconstructed local adsorption geometries, depending on whether they were located within the forward scattering cone[24], cf. Fig. 1(b). The implied necessity of combining several (at least two) data sets taken at different angles of incidence to deduce the complete 3D surrounding of the beam-splitter[25] could be overcome with the introduction of an improved reconstruction algorithm proposed by Saldin and Chen[11].

This *Compensated Object and Reference wave Reconstruction by an Energy-dependent Cartesian Transform* (CORRECT)[11] allows the calculation of the real space distribution around the adsorbate $|B(\mathbf{r})|^2$ (where $\mathbf{r} \equiv (\mathbf{r}_\parallel, z)$ is a position vector relative to the origin at the adsorbate with components $\mathbf{r}_\parallel$ parallel to, and z perpendicular to the surface) via the following expression:

$$B(\mathbf{r}) = \iint_{\mathbf{k}_\parallel} \left[\int_{k_\perp} K(\mathbf{k}_\parallel, k_\perp; \mathbf{r}) \chi(\mathbf{k}_\parallel, k_\perp) e^{-(ikr - k_\perp z)} dk_\perp \right] e^{i\mathbf{k}_\parallel \cdot \mathbf{r}_\parallel} d^2\mathbf{k}_\parallel. \quad (2.1)$$

Note, that in contrast to previous reconstruction algorithms that performed the involved 3D integral in a polar coordinate system (angle and energy), the data input is provided on a cartesian grid $(\mathbf{k}_\parallel, k_\perp)$, which will be of importance when discussing the step towards ordered superstructures in the next section.

The transform does not operate directly on the measured intensities H, but rather on a contrast-enhancing and normalizing function

$$\chi(\mathbf{k}_\parallel, k_\perp) = \frac{H(\mathbf{k}_\parallel, k_\perp) - H_{av}(\mathbf{k}_\parallel)}{H_{av}(\mathbf{k}_\parallel)} \quad (2.2)$$

with

$$H_{av}(\mathbf{k}_\parallel) = \frac{\int H(\mathbf{k}_\parallel, k_\perp) dk_\perp}{\int dk_\perp}. \quad (2.3)$$

It has been shown theoretically that the use of such a χ-function helps to partially remove the self-interference terms $|R(\mathbf{k})|^2$ and $|O(\mathbf{k})|^2$ in the DLEED intensity, which give rise to spurious high values of the real space distribution $|B(\mathbf{r})|^2$ in the vicinity of the origin[11]. Additionally, χ has been designed in such a way as to suppress modulations in the DLEED patterns that arise from some partial ordering among the adsorbates[13].

The last part in the expression to be described is the integral kernel which corrects for the anisotropy of the reference wave. In a zeroth order approximation it can be written

$$K(\mathbf{k}_\parallel, k_\perp; \mathbf{r}) = \left[\frac{f_a(\mathbf{k}_i \cdot \hat{\mathbf{r}}) + C}{r} \right]^{-1}. \quad (2.4)$$

Here $f_a(\mathbf{k}_i \cdot \hat{\mathbf{r}})$ is the atomic scattering factor of the adsorbate, $\hat{\mathbf{k}}_i$ the direction of electron incidence, and C the so called kernel constant (which we take to be real), and which represents an isotropic approximation to the backscattering by the substrate prior to scattering by the adsorbate. Optimizing the value of C provides access to those atoms of the local adsorption geometry that lie outside the forward scattering direction of the beam-splitter[26]. This allows the retrieval of the complete 3D surrounding of the latter from data of normal incidence alone. The algorithm in this present form has been shown to give reliable images using theoretical[11,26], as well as experimental DLEED data[12,13].

III. SPOT INTENSITIES VERSUS DIFFUSE DISTRIBUTIONS

The original holographic reasoning[9] was based on the assumption that only one beam-splitting adsorbate atom is present on the substrate surface. With several such adsorbates, each time in the same local structure but without long range order among them (lattice gas disorder), intensities simply add up in the low coverage limit leaving the resulting diffuse distribution practically unchanged[10,27]. A different situation emerges with the onset of order at higher coverages and/or upon thermal annealing: additional modulations in the DLEED pattern are created that eventually cause the breakdown of the holographic algorithm[13].

For the case of a completely ordered superstructure of such adsorbates, the modulations caused by the lattice factor concentrate the diffuse intensities to a series of discrete superstructure - or fractional order - spots when the unit mesh of the adsorbate layer is larger than that of the crystalline substrate. However, the simultaneous extinction of diffuse intensity between the spots as caused by destructive interference between the waves originating from different adsorbate-substrate clusters, does not remove the crystallographic information wanted: the energy dependence of the superstructure spot intensities is the same as the one displayed by the corresponding $\mathbf{k}_\parallel$-positions in a diffuse distribution resulting from a disordered adlayer in the equivalent local adsorption geometry[28]. The only restriction is that scattering between such clusters has to be negligible, a condition satisfied even for relatively small superstructures when using normal incidence data[29,30].

So, even though the perfect order among the adsorbates significantly reduces the amount of available data, the few remaining intensities are not masked by disturbing modulations as in the case of partial disorder inhibit-

ing the final $\mathbf{k}_\parallel$-integration in equation (2.1). The superstructure spots can be thought of as sampling the DLEED intensity distribution of the corresponding lattice gas on a finite grid. Therefore, as suggested earlier[30], a DLEED holographic algorithm may in principle be applied to such ordered superstructure systems with the only difference of a reduced density of input data in $\mathbf{k}_\parallel$. This makes more apparent, why the CORRECT algorithm is so particularly suited for the extension to ordered phases: the data is provided on the appropriate cartesian grid and only normal incidence is required. Interestingly, earlier investigations on the information content of diffuse intensities[28], as well as on the minimum data base of the algorithm[26], showed, that the continuous diffraction distribution resulting from disordered atomic adsorbates is already sufficiently described when using a (3×3) sampling grid. Information on a denser grid is largely redundant. Hence, there are no drastic changes to be expected when making the transition from disordered systems to phases with large superstructure cells like the (3×3) reconstruction of SiC(111) of the present paper. This allows us to apply the algorithm developed for DLEED without any modifications. However, it should be emphasized, that a further reduced data base in connection with superstructures smaller than a (2×2) can lead to aliasing effects in the Fourier-like transform due to insufficient sampling[15].

The application of LEED holography to ordered surfaces involves several practical advantages. For the diffraction process it is irrelevant, whether the beam-splitter is an externally adsorbed atom or intrinsically belongs to the surface. Thus, besides ordered adsorption systems now also ordered substrate reconstructions can be investigated. Additionally, the measurement of discrete spot intensities is much less delicate than that of the diffuse intensities which are comparatively weak. The high signal-to-noise ratio of the bright spots allows easy subtraction of contributions due to thermal diffuse scattering. Also, at higher energies fractional spot intensities are not that much influenced by cross-talk from the bright substrate spots as is the case for diffuse intensities[10,30]. Furthermore, holographic LEED seems also suitable to tackle larger unit cell reconstructions: the high number of fractional order spots generated in these cases provides a fine sampling grid and ensures the proper working of the integral transform. However, practical reasons also commend an upper limit for the unit cell size as the increasing number of closely spaced spots impairs a proper data acquisition, especially at higher energies where more and more spots appear and weak spots are disturbed by their bright neighbours. A unit cell such as the (7×7) on Si(111)[31,32] is probably already too large from an experimental point of view as the accessible energy ranges become too small.

In addition, it becomes more and more unlikely that such a large unit cell contains only one elevated adatom (the Si(111)-(7×7) actually contains 12 adatoms). This would violate the strongest restriction of the technique at its current stage, i.e. the condition that only a single beam-splitter is allowed within each unit cell. Several such prominent atoms per unit cell would lead to intermixing of their respective contributions as will be demonstrated further below. This is all the more problematic, since the actual number of elevated adatoms is just one of the quantities sought in the structure analysis of an *a priori* unknown surface (even though STM might help as in the present case). Future efforts in methodologic improvements should hence be directed to overcome the multiple beam-splitter problem, which did not occur in the previous applications to simpler diffuse or ordered systems. As a consequence, until there is a proper theoretical description of the detailed influences on the reconstructed images, the systems to which holographic LEED is to be applied have to be chosen with considerable care.

IV. RECONSTRUCTION USING EXPERIMENTAL DATA

SiC is a material that displays most suitable electronic properties which have made it a promising candidate for high power and high frequency devices. Particularly, the (3×3) phase of the SiC(111) surface has drawn considerable interest in the last years, caused by the observed crystal growth improvement[33], that is achieved when this reconstruction is stabilized under highly Si-rich conditions[16]. Its complexity, which can already be deduced from an extensive debate in the literature[18–20,34], had hitherto prevented a detailed structure analysis using trial-and-error methods. However, the high number of fractional order spots caused by such a comparatively large surface unit cell makes this phase an ideal candidate for a holographic investigation in view of the reasoning outlined above.

The cubic 3C-SiC polytype was chosen, since its (111) oriented surface exposes only one definite stacking sequence[35], i.e. there is no coexistence of domains of different orientation, which would have to be expected in the case of hexagonal polytypes with different layer stackings possible at the surface[35], and which would certainly complicate if not inhibit the interpretation of the reconstructed images. Additionally, there is strong evidence from comparison of experimental LEED intensities[22], as well as from DFT test calculations[36], that the atomic structure of the (3×3) surface phase itself is rather independent of the sample polytype. So, results obtained for 3C-SiC(111) can be expected to hold also for other polytypes.

LEED I(V)-curves of the sharp diffraction pattern were measured in the energy range 50-300 eV using normal electron incidence. Details on the data acquisition and sample preparation will be published elsewhere[22,37]. The low diffuse background and noise level allowed the recording of 14 fractional order beams closest to specular reflection, which are symmetry-inequivalent at normal incidence. Providing the measured intensities as input to

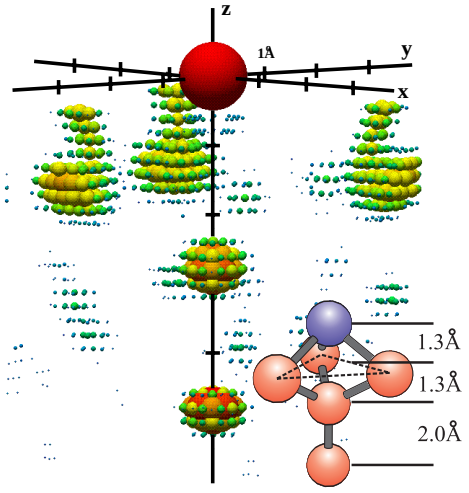

FIG. 2. Recovered local geometry of the SiC(111)-(3×3) structure using experimental data in the energy range 50-300 eV and kernel constant $C = 2.7$ Å. The maximum noise level in the image is 48 % of the maxima denoting the atom positions (noise cut-off: 25 %). For details on the display procedure, see Section IV. The inset displays a schematic of the retrieved adcluster geometry including chemical bonds and the approximate layer distances as determined by holographic LEED.

expression (2.1) resulted in the 3D image displayed in Fig. 2: the real-space distribution $|B(\mathbf{r})|^2$ is calculated on a grid of 0.2 Å resolution inside a cylinder of depth 6.0 Å and a lateral radius 3.0 Å, which is consistent with estimates on the lateral validity of the algorithm[15]. Small spheres are drawn at the grid points, indicating the reconstructed real-space intensity by their diameter which scales linearly with the intensity. As pointed out in previous holographic investigations[11–13,26], this type of display permits a quick understanding of the essential features of the structural unit determined holographically and will therefore be used in all figures included in the present paper.

The origin of the coordinate system is defined by the beam-splitter, which is artificially added in the image as a black sphere to facilitate understanding. The highly Si-rich conditions under which the (3×3) phase is observed suggest this beam-splitter to be Si, the scattering factor of which is consequently used for the computation of the integral kernel (2.4). However, the zeroth order approximation of the latter is most sensitive only to the essential form of the atomic scattering factor, which is very similar for most elements. Using carbon as a beam-splitter in the computation consequently did not change the resulting images considerably. The kernel constant C in this expression is optimized such that all atoms in the geometry appear with approximately equal brightness[26]. The highest disturbing intensity at non-atomic positions (henceforth referred to as noise level) is with 48 % of the overall maximum value at an unprecedented low level. This has to be attributed to the – in comparison to the DLEED case – much better quality of conventional LEED I(V) data and the increased energy range available.

The image allows the unambiguous identification of the local adcluster geometry formed by an adatom supporting trimer and two further atoms vertically below the beam-splitter (see inset in Fig. 2). The rough layer distances of 1.3 Å (adatom-trimer), 1.3 Å (trimer and first lower atom) and 2.0 Å (between lower atoms) correspond surprisingly well with the (7×7) DAS model of the Si(111) surface[32]. This already indicates that probably the complete retrieved geometry corresponds to Si atoms on top of the SiC substrate. Note, that the distorted form of the trimer atoms is an effect of the scattering factor in connection with the zeroth order approximation of this property in the integral kernel (2.4)[11]. However, neither the obtained spatial resolution, nor the exact position of the atoms inside the geometry are the primary object or strength of the holographic analysis: it is rather the direct and quick idea of a structural unit belonging to the investigated surface.

The obtained tetramer formed by the adatom and the supporting trimer is typical for hexagonal semiconductor surfaces. Its unambiguous determination in the holographic image proves that only one of the two possible orientations rotated by 60° with respect to each other is present on the surface. This already excludes domains of differently rotated, i.e. coordinated clusters, as can also directly be deduced from the pronounced threefold symmetry of the measured fractional order spot intensities[22,37]. It further rules out the model proposed first by Kaplan[34] of a (3×3) mesh which in close analogy to the (7×7) DAS model[32] contains two such tetramers per surface unit cell, which in turn would necessarily be differently oriented. It should be noted, that this model was also inconsistent with STM investigations, which clearly revealed only one elevated protrusion per unit cell, thus strongly favouring models including a single tetramer[18–20]. Since the atomic beam-splitter has to be identified with the top adatom of this tetramer, exactly these results ultimately enabled the application of LEED holography to this structure: the obligatory uniqueness of the beam-splitter excludes DAS-like models with two tetramers per surface unit cell from the class of systems accessible under the current state of theory.

We should recall now that we are dealing with an *a priori* unknown structure. Although the low noise level in the image may appear very convincing, it has to be recognized that the strong multiple scattering combined with the anisotropic scattering factors for low energy electrons may lead to serious artefacts in the images that would not easily be distinguishable from real atoms. Since the multi-energy algorithms developed for holographic LEED can only suppress, but not completely eliminate these effects, it is often advisable to vary the used input energy

range. In view of the fact that scattering factor anomalies may sometimes even lead to an increased image quality when reducing the number of included energies, the stability of the obtained result under such variations can significantly increase the confidence in the deduced local geometry. Dividing the experimental data into various subsets always resulted in equivalent images, which strongly confirms the structural unit determined. In general, one has to admit that the weak scattering power of light elements like Si and C might provide a favourable case for holography as multiple scattering contributions are expected to be smaller than for example for transition metal crystals. However, recent results for the system O/Ni(001)-p(2x2)[15] make us believe, that the developed algorithm does also work for stronger scattering materials. Now, although the experimental result appears convincing a test of the validity and sensitivity of the method seems adequate, which is presented in the next sections using simulated intensities from various fictitious models.

V. VERTICAL SENSITIVITY AND STACKING OF DEEPER LAYERS

The simplest model consistent with the atomic positions obtained from the holographic reconstruction would be just an adatom on top of a SiC bilayer. Yet, such a model appears improbable since it would not account for the strong silicon enrichment at the surface as detected by earlier Electron Energy Loss (EELS) and Auger Electron Spectroscopy (AES) results[34], which we discuss in detail elsewhere[22]. Assuming therefore the tetramer as the essential structural unit – presumably formed by Si atoms in view of the EELS and AES results – the first question to be verified is its position on the underlying substrate. The simplest possible solution would be to directly place it somehow on top of the SiC sample, to which the two further atoms showing up in the holographic reconstruction would then belong. Given the bilayer stacking sequence of this material in the [111] direction it is, however, impossible to find any location consistent with two atoms directly on top of each other as predicted by Fig. 2. Even though the holographic method is most reliable in just this direction vertically below the beam-splitter, in which atoms show up already without the scattering factor compensation by the integral kernel (2.4), there is yet no definite certainty on the limit of the algorithm's validity for deeper layers: all previous investigations with DLEED data had dealt with rather simple test structures, which were already completely determined by the atomic positions in the first two layers. Hence, the now performed calculation of $|B(\mathbf{r})|^2$ up to a depth of 6.0 Å raises concerns whether the lowest lying atom identified at 4.6 Å might already be outside such a limit.

Consequently, for the moment we focus on only the tetramer and the third layer atom of the holographic image. This arrangement suggests a cluster position in which each of the three trimer atoms is located in a hollow site of the topmost hexagonal bilayer of the SiC substrate. Depending on whether this position is fourfold coordinated, i.e. on top of a carbon atom in the substrate bilayer (T4 site) or truely threefold coordinated (H3 site), the tetramer would have to be oriented as in the SiC substrate bilayers or rotated by 60°, respectively. The adatom would then reside on top of a Si atom in the bilayer, which corresponds to the third layer atom of the holographic image. No further atom would be present 2 Å below the latter in either site geometry. Note, that this geometry corresponds to the model proposed by Li and Tsong on the basis of their STM work[19], which assumed such coordinated tetramers in a (3×3) periodicity directly on top of the SiC. In order to verify whether the atom additionally appearing in Fig. 2 is an algorithmic artefact or not, we thus simulated theoretical LEED I(V) curves of an adcluster model for the identical number of fractional order beams and the same energy range as in the experiment (details of these calculations will be published elsewhere[22]). In order to focus on the depth information available from LEED holography we chose the fourfold coordinated trimer atom positions, yet artificially expanded the distance between adcluster and substrate to push the third layer atom to a position 3.2 Å below the beam-splitter. A schematic view of this geometry can be seen in the inset of Fig. 3. The resulting holographic image is displayed in Fig. 3, showing the ex-

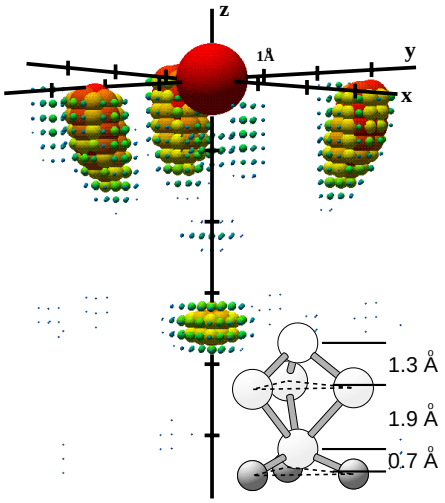

FIG. 3. Same as Fig. 2, but using simulated I(V) curves of a simplified Li/Tsong model as described in section V. The electron energy range was 146-300 eV, the kernel constant $C = 5.0$ Å and the maximum noise level is at 46 % of the maxima at the atom positions (noise cut-off: 25 %). The inset displays the atomic arrangement in the model assumed to calculate the intensities used for the holographic reconstruction.

pected tetramer unit plus the third layer atom, but also consistently not indicating any sign of possible artefacts vertically below the adatom. Only the carbon atoms of the substrate SiC bilayer are still within the reconstruction volume, but do not appear in the reconstructed image (Fig. 3). However, one has to consider that in the geometry chosen they are 4.3 Å apart from the beam-splitter and 1.9 Å off the vertical axis, and in addition represent comparatively weak scatterers. This distance – not in forward scattering direction – probably represents the detection limit at least for a weak scatterer. However, in view of the absence of artefacts in the holographic image obtained for our test model, the presence of two atoms vertically below the adatom as indicated in the real space reconstruction from the experimental data has to be assumed correct. Furthermore, the pronounced appearance of the lowest atom might indicate that it is silicon since a weakly scattering C atom should not be detectable at that depth. Our test case resulting in the image shown in Fig. 3 thus clearly rules out the possibility of the Li/Tsong model, whose bilayer stacking sequence results in fourth layer atoms off the vertical axis and which is thus incompatible with the lowest atom in the image obtained from the experimental data.

This further emphasizes the importance of the retrieval of the two deepest atoms in the local geometry. Since only small deviations from the bulk positions are usually to be expected in such deep layers, the location of each of these atoms uniquely determines the complete stacking sequence of the corresponding entire layer. Hence, even though the obtained structural unit itself may contain only a small number of atoms, its consistent embedding into the surface unit cell subsequently can reveal a quite important further fraction of the investigated surface.

VI. CAN A VACANCY ACT AS A BEAM-SPLITTER?

The confirmation of the lowest atom inside the revealed structural unit, whose on top stacking is inconsistent with a SiC bilayer at the very surface, necessitates to include an additional Si adlayer in the crystallographic model. Such an adlayer between tetramer and substrate had already been included in the original DAS-like model, since the EELS and AES results indicated the strong presence of Si-Si bonding in the highly Si-rich surface[34]. In order to bring this otherwise very reasonable model in accordance with the STM data described above, Kulakov *et al.* proposed the absence of one of the two tetramers per surface unit cell[18]. In the language of the DAS-type models the top atom of the trimer represents an adatom on top of a Si bilayer. In the DAS-unit cell one of the two adatoms is located on a piece of bilayer in faulted orientation as indicated in Fig. 4(a). One would expect an energetical difference between the adcluster which follows the substrate stacking direction and the one, which introduces

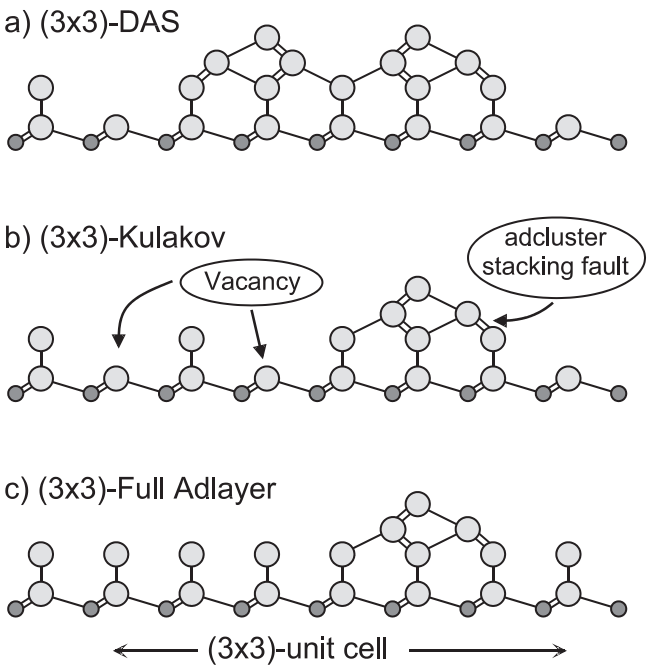

FIG. 4. Schematic side view of different models for the SiC(111)-(3×3) reconstruction in a projection parallel to the [1$\bar{1}$0]-plane (Si atoms are depicted by large spheres, C atoms by small darker spheres. Bonds within the projection plane are drawn as single lines, double lines represent two bonds pointing out of the projection plane by +60° and -60°, respectively.) a) DAS-model containing two adatoms and one cornerhole per unit cell as proposed by Kaplan[34]. b) Single adatom model containing two cornerholes with a local stacking fault in the Si-bilayer fragment underneath the adatom; derived from the model by Kulakov et al. without the stacking fault[18], c) Single adatom-trimer-cluster residing on a complete monolayer in (1×1) periodicity with all cornerholes filled. The bilayer fragment underneath the adatom again represents a local stacking fault.

a local stacking fault in the adlayer. Thus it is plausible that in the end exclusively the more favourable type would be present on the surface. Such a model, hence including only a single tetramer with definite orientation in each (3×3) unit cell, could explain not only the single protrusion in the STM images, but also the threefold symmetry of the LEED pattern. What remains, is the question which of both orientations is actually realized. Note, that the orientation of the adcluster can be deduced from a comparison with a previous LEED analysis of the (1×1) phase on the same sample[21,35,38]. However, we demonstrate a verification of this assignment using test calculations, a method that could generally be applied in cases where no independent analysis of the substrate is available.

Both Kulakov-type models, with the adcluster either introducing or not introducing a local stacking fault, comply with the holographic image from the experimental data, when identifying the upper of the bottom two

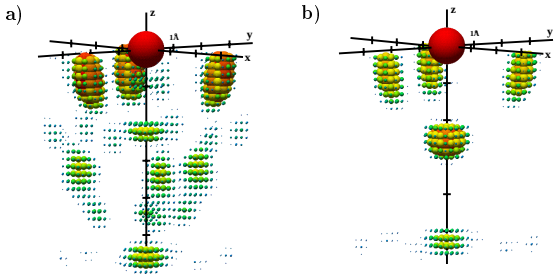

FIG. 5. Same as Fig. 2, but using simulated I(V) curves of a simplified Kulakov model as described in section VI. The electron energy range was 146-300 eV and the kernel constant $C = 5.0$ Å. a) geometry including cornerholes in the Si adlayer, cf. Fig. 4(b): maximum noise level at 76 %, b) geometry with filled cornerholes in the Si adlayer, cf. Fig. 4(c): maximum noise level is at 29 % (noise cut-off: 25 %).

atoms as belonging to the Si adlayer and the other one as a Si atom of the substrate's topmost bilayer. Yet, the subsequent interplay between LEED holography and conventional LEED can do better than that: when reconstructing images using theoretically simulated data, the orientation of the substrate inside the given coordinate system is known. Depending on the resulting orientation of the adcluster in the image – or to be exact, the tetramer of four atoms representing the Si bilayer underneath the adatom – when choosing one of the two equivalent beam assignments in the LEED pattern, its orientation with respect to the bulk can be deduced even without seeing the latter in the reconstructed image itself. From the result shown in Fig. 3, we therefore know the orientation of an unrotated tetramer. Comparing this with the holographic image obtained from the experimental data (cf. Fig. 2) we find that the adcluster geometry involves a local stacking fault of the Si bilayer as shown in Fig. 4(b). Hence, of all the previously existing models of the SiC(111)-(3×3) phase, LEED holography would only be fully consistent with the Kulakov model in the local stacking fault version.

In order to further verify this conclusion, we simulated LEED I(V) curves for this model, whereby, however, small deviations from bulk-like positions as for example induced by dimerization were not considered. Surprisingly, the corresponding holographic image displayed in Fig. 5(a) is of considerably worse quality than the previous results. Although all five atoms of the expected structural unit show up, their overall configuration is badly distorted and high noise in form of three concentrated artefacts prevents the unambiguous distinction between real atoms and false contributions. Since the image from ideal theoretical data should only be better than the one from the experiment, the situation in the latter has somehow to be more favourable for LEED holography than so far assumed, which, of course, demands clarification.

As mentioned above, a severe source of an algorithmic breakdown at its current level of development is given by the multiple beam-splitter problem. Therefore, we reconsidered the atomic arrangement of the Kulakov model under this point of view. Since it was derived in close analogy to the DAS model, its Si adlayer is not completely closed but contains vacancies to relax the stress induced by the lattice mismatch[18]. These so called cornerholes appear just like in the Si(111)-(7×7) structure[32] and break the (1×1) periodicity as much as the identified beam-splitting atom on top of the tetramer. Consequently one might also concede them the *same* holographic interpretation. In the sketch of the Kulakov model in Fig. 4(b) it can be seen that the vacancy is even enlarged by the removal of one adcluster from the DAS model, cf. Fig. 4(a). It may appear difficult at first glance to imagine a vacancy as a possible beam-splitter, but speaking in terms of missing wave contributions to achieve the destructive interference corresponding to a perfect (1×1) adlayer helps to understand its influence on the fractional order beams. This would be equivalent to replacing the vacancy by a pseudo-adatom with the same dynamic scattering behaviour.

From this point of view, we would have to conclude that the Kulakov model contains various distinct beam-splitters per surface unit cell, whose respective wave contributions could consequently interfere and completely prohibit a holographical interpretation. However, the strong damping of the low energy electrons makes us hope, that the dominant contribution in the reconstructed image is due to the most elevated, periodicity breaking atom in the surface unit cell and that the existence of further extra atoms or vacancies in the superstructure unit cell leads "only" to image disturbances although they might be considerable. This interpretation would help to understand why Fig. 5(a) basically shows the local environment of the top tetramer atom plus artefacts and some distortions that may then be due to the cornerhole vacancies. To test this line of thought, we simulated LEED I(V) data of exactly the same model as before, but filling the vacancies with Si atoms at bulk-like positions in the Si adlayer as shown in Fig. 4(c). The resulting image in Fig. 5(b) is of impressive clarity and contains all essential features of the result obtained with the experimental data. We take this as a strong indication of the correctness of our reasoning, although we want to stress again that there is yet no *proper* theoretical treatment of the multiple beam-splitter difficulty in LEED holography. It should further be noted that in our test model, cf. Fig. 4(c) we only filled the Si monolayer. The adatom supporting trimer atoms are still not repeated with the bulk periodicity and thus break the (1×1) periodicity, too.

VII. INFLUENCE OF SUBSTRATE RECONSTRUCTIONS

What had started as a pure necessity to ensure the correct working of the holographic algorithm, subsequently turned out to be the last required piece for the solution of the (3×3) puzzle. Since LEED holography seemed only fully consistent with a Kulakov-derived model containing one tetramer in local stacking fault orientation on a closed Si adlayer without cornerholes, a careful reconsideration then showed that indeed there had been no other reason for including the cornerholes at first hand but the sole analogy to the DAS model. The situation for SiC(111)-(3×3), where the Si adlayer shows an intrinsic lattice mismatch of 20 % with respect to the underlying substrate, might however require a different form of relaxing the lattice strain under simultaneous dangling bond saturation than the cornerhole and dimerization principle underlying the homoepitactic Si(111)-(7×7). As a further hint, the obtained STM images of the (3×3) phase[20,21] never showed comparably strong cornerhole depressions as visible on the silicon surface[39].

Consequently, the thus most favoured model with filled cornerholes was input to a refining LEED and Density Functional Theory (DFT) analysis. Even though the holographic results had considerably reduced the multiparameter space for the trial-and-error search of both methods, it should however be emphasized that the remaining structure determination was still a tremendous task: there is a qualitative difference between a coarse local beam-splitter surrounding that depicts a small fraction of the huge surface unit cell and a detailed variation of all involved atomic positions on a dense grid in steps of a few hundredths of Ångstrøms. It was in this respect most gratifying that both analyses independently yielded the same full (3×3) structure by input of the holographically recovered cluster: the resulting final *twist* model[21] can indeed essentially be described as a SiC substrate with a strongly buckled Si adlayer without any cornerholes plus one tetramer per surface unit cell consisting of a trimer and one adatom. These trimer atoms and the Si adlayer below locally resemble a Si bilayer in stacking fault orientation. A more detailed description of the exact model and both analyses involved will be given elsewhere[22,40].

Yet, we have to realize that the bond optimizing relaxations inside the adlayer also contribute to the superstructure spot intensities and might consequently affect the working of the holographic reconstruction algorithm: each atom, that has left its (1×1)-like position, has in principle to be regarded as a possible additional beam-splitter in view of the discussion in section VI. Therefore, as a final test, we used the I(V) curves calculated for the exact geometry of the optimized model as input to the holographic algorithm. The resulting image is displayed in Fig. 6 and shows exactly the same local adatom environment as the experimental data, which we - even in the presence of buckling – take as a final proof of the validity of our new method. In accordance with the experience made recently with other, simpler structures[15], the effect of the slight deviations from bulk-like positions on the reconstructed image is apparently negligible and leads only to an increased overall noise level, which can be seen comparing Fig. 5(b) and Fig. 6, whose underlying structure differs exclusively by just these substrate relaxations. All this becomes more understandable, when recalling, that it is again only the *difference* in the outgoing wavelets arising from buckled atoms that can act as a conduit for diffraction intensity in the fractional order beams. The (additionally damped) contributions due to these shifts can hence be regarded small with respect to the major rupture of periodicity caused by the introduction of a completely new and elevated atom such as the adatom in the present structure. In this context, it is also important to notice, that the majority of such shifts is far below the resolution capabilities of LEED holography at its present stage, which can typically be stated to be ≈ 0.6 Å.

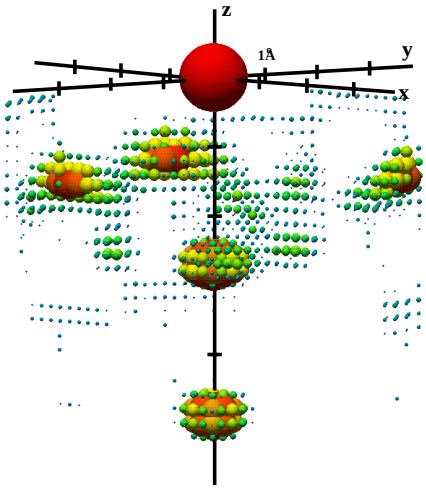

FIG. 6. Same as Fig. 2, but using simulated I(V) curves of the final twist model as described in section VII. The electron energy range was 65-300 eV, the kernel constant $C = 0.75$ Å and the maximum noise level is at 51 % (noise cut-off: 25 %).

VIII. CONCLUSION

In the present paper we described in detail the contribution that holographic LEED can provide, when applying it to a complex superstructure. Using a holographic interpretation of fractional order spot intensities, a 3D image of the local geometry around an elevated, periodicity breaking adatom can be retrieved. The structural unit thus obtained has to be consistent with the real space

atomic structure and can be used to considerably reduce the multi-parameter space and possibly enable the trial-and-error search of geometry optimizing methods like quantitative LEED and DFT energy minimization. We exemplified this for the case of the SiC(111)-(3×3) phase, where the holographically derived adcluster *directly* rules out the majority of all previously existing models of this surface and whose geometry has now been fully confirmed by the final *twist* model obtained independently by conventional LEED and DFT. This application additionally marks the first example that a holographic inversion of LEED data actually played a crucial part in the determination of a complex and *a priori* unknown structure.

We have illuminated the power and the limits of this new holographic LEED method for ordered surfaces. Even in the best of all cases the obtained image is restricted to the local geometry around the prominent beam-splitter. Only for very simple surfaces, this uniquely determines all atomic positions inside the unit cell. Furthermore, exclusively for such simple test surfaces has this still developing method been thoroughly tested so far. There, some severe problems like the multiple beam-splitter problem encountered in the present investigation do usually not arise and have therefore not yet been theoretically treated. Consequently, the systems, to which holographic LEED is to be applied, have for the moment to be chosen with great care.

Nevertheless, regarding the immense problems that quantitative LEED and DFT face with complex, large superstructure systems, every directly obtainable pre-information is highly welcome. In this view, the possibility of a holographic approach raises hopes that a new ally in the structure analysis of these ordered phases has been found. It is particularly its *direct* simplicity that already now renders holographic LEED such an ideal supplement to its established trial-and-error brethren, even though the young method has still a long way to go.

ACKNOWLEDGEMENTS

The authors are indebted to Prof. D.K. Saldin and Dr. P.L. de Andres for many helpful discussions. This work was supported by Deutsche Forschungsgemeinschaft (DFG) in particular through SFB 292.

---

[1] NIST Surface Structure Database 2.0 (1995), Nat. Inst. Stand. Technol., Gaithersburg (USA).

[2] J. B. Pendry, *Low Energy Electron Diffraction*, Academic Press, London, (1974); M. A. Van Hove, W. H. Weinberg, and C.-M. Chan, *Low Energy Electron Diffraction*, Springer-Verlag, Berlin (1986).

[3] M. A. Van Hove and S. Y. Tong, *Surface Crystallography by LEED*, Springer-Verlag, Berlin, (1979).

[4] K. Heinz, Rep. Prog. Phys. **58**, 637 (1995).

[5] P. J. Rous, Surf. Sci. **296**, 358 (1993); R. Döll and M. A. Van Hove, Surf. Sci. **355**, L393 (1996); M. Kottcke and K. Heinz, Surf. Sci. **376**, 352 (1997); M. A. Van Hove, W. Moritz, H. Over, P. J. Rous, A. Wander, A. Barbieri, N. Materer, U. Starke, and G. A. Somorjai, Surf. Sci. Rep. **19**, 191 (1993).

[6] J. B. Pendry, K. Heinz, and W. Oed, Phys. Rev. Lett. **61**, 2953 (1988); J. B. Pendry and K. Heinz, Surf. Sci. **230**, 137 (1990).

[7] A. Szöke, *Short Wavelength Coherent Radiation: Generation and Applications*, AIP Conf. Proc. No. **147**, edited by D. J. Attwood and J. Boker (New York, 1986).

[8] J. J. Barton, Phys. Rev. Lett. **61**, 1356 (1988).

[9] D. K. Saldin and P. L. De Andres, Phys. Rev. Lett. **64**, 1270 (1990).

[10] U. Starke, J. B. Pendry, and K. Heinz, Prog. Surf. Sci. **52**, 53 (1996).

[11] D. K. Saldin and X. Chen, Phys. Rev. B **52**, 2941 (1995).

[12] D. K. Saldin, K. Reuter, P. L. De Andres, H. Wedler, X. Chen, J. B. Pendry, and K. Heinz, Phys. Rev. B **54**, 8172 (1996).

[13] D. K. Saldin, X. Chen, J. A. Vamvakas, M. Ott, H. Wedler, K. Reuter, and K. Heinz, Surf. Rev. Lett. **4**, 991 (1997).

[14] K. Reuter, J. Bernhardt, H. Wedler, J. Schardt, U. Starke, and K. Heinz, Phys. Rev. Lett. **79**, 4818 (1997).

[15] K. Reuter, J. A. Vamvakas, D. K. Saldin, V. Blum, M. Ott, H. Wedler, R. Döll, and K. Heinz, Phys. Rev. B, *in press.*

[16] S. Tanaka, R. S. Kern, and R. F. Davis, Appl. Phys. Lett. **65**, 2851 (1994); A. Fissel, B. Schröter and W. Richter, Appl. Phys. Lett. **66**, 3182 (1995).

[17] see e.g. the complete issue phys. stat. sol. (b) **202** (1997) dedicated to SiC.

[18] M. A. Kulakov, G. Henn, and B. Bullemer, Surf. Sci. **346**, 49 (1996).

[19] L. Li and I. S. T. Tsong, Surf. Sci. **351**, 141 (1996).

[20] U. Starke, J. Schardt, and M. Franke, Appl. Phys. A **65**, 587 (1997).

[21] U. Starke, J. Schardt, J. Bernhardt, M. Franke, K. Reuter, H. Wedler, K. Heinz, J. Furthmüller, P. Käckell, and F. Bechstedt, Phys. Rev. Lett. **80**, 758 (1998).

[22] J. Schardt, J. Bernhardt, M. Franke, K. Reuter, U. Starke, and K. Heinz, Phys. Rev. B, *to be published.*

[23] S. Y. Tong, Hua Li and H. Huang, Phys. Rev. Lett. **67**, 3102 (1991); J. J. Barton, Phys. Rev. Lett. **67**, 3106 (1991).

[24] C.-M. Wei and S. Y. Tong, Surf. Sci. **274**, L577 (1992).

[25] C.-M. Wei, S. Y. Tong, H. Wedler, M. A. Mendez, and K. Heinz, Phys. Rev. Lett. **72**, 2434 (1994); K. Heinz and H. Wedler, Surf. Rev. Lett. **1**, 319 (1994).

[26] K. Reuter, H. Wedler, M. Ott, K. Heinz, J. A. Vamvakas, X. Chen, and D. K. Saldin, Phys. Rev. B **55**, 5344 (1997).

[27] J. B. Pendry and D. K. Saldin, Surf. Sci. **145**, 33 (1984).

[28] K. Heinz, U. Starke, and F. Bothe, Surf Sci. Lett. **243**, L70 (1991); K. Heinz, U. Starke, M. A. Van Hove, and G. A. Somorjai, Surf. Sci. **261**, 57 (1992).

[29] S. Y. Tong, M. A. Van Hove and B. J. Mrstik, in Proc. 7th Intern. Vacuum Congr. and 3rd Intern. Conf. on Solid Surfaces (Vienna, 1977), p.2407; K. Heinz and G. Besold,

Surf. Sci. **125**, 515 (1993).
[30] M. A. Mendez, C. Glück, and K. Heinz, J. Phys. Cond. Mat. **4**, 999 (1992); M. A. Mendez, C. Glück, M. Wagner, U. Löffler, R. Döll, and K. Heinz, Surf. Sci. **290**, 45 (1993).
[31] S. Y. Tong, H. Huang, C. M. Wei, W. E. Packard, F. K. Men, G. Glander, and M. B. Webb, J. Vac. Sci. Technol. A **6**, 615 (1988).
[32] K. Takayanagi, Y. Tanishiro, M. Takahashi, and S. Takahashi, Surf. Sci. **164**, 367 (1985);
[33] H. S. Kong, J. T. Glass, and R. F. Davis, J. Appl. Phys. **64**, 2672 (1988); T. Kimoto and H. Matsunami, J. Appl. Phys **76**, 7322 (1994).
[34] R. Kaplan, Surf. Sci. **215**, 111 (1989).
[35] U. Starke, phys. stat. sol. (b) **202**, 475 (1997); J. Schardt, J. Bernhardt, U. Starke, and K. Heinz, Surf. Rev. and Lett. **5**, 181 (1998).
[36] F. Bechstedt, P. Käckell, A. Zywietz, K. Karch, B. Adolph, K. Tenelsen, and J. Furthmüller, phys. stat. sol. (b), 35 (1997).
[37] J. Bernhardt, M. Franke, J. Schardt, U. Starke, and K. Heinz, *to be published*.
[38] U. Starke, J. Bernhardt, M. Franke, J. Schardt, and K. Heinz, Diamond and rel. mat. **6**, 1349 (1997).
[39] R. S. Becker, J. A. Golovchencko, D. R. Hamann, and B. S. Swartzentruber, Phys. Rev. Lett. **55**, 2032 (1985); R. J. Hamers, R. M. Tromp, and J. E. Demuth, Phys. Rev. Lett. **56**, 1972 (1986).
[40] J. Furthmüller, P. Käckell, and F. Bechstedt, *to be published*.